32nd URSI GASS, Montreal, 19–26 August 2017

Irregular-Grid-Based Particle-in-Cell Simulations of Resonant Electron Discharges with Probabilistic Secondary Electron Emission Model

Dong-Yeop Na[(1)], Yuri A. Omelchenko[(2)], and Fernando L. Teixeira[(1)]
(1) ElectroScience Laboratory, The Ohio State University, Columbus, OH 43212 USA
(2) Trinum Research Inc., San Diego, CA 92126 USA

Abstract

Resonant electron discharges (mutlipactor effects) in vacuum electronic devices are investigated through irregular-grids-based particle-in-cell (PIC) simulations. The Furman probabilistic model for the secondary electron emission (SEE) is embodied in a PIC algorithm that yields a self-consistent time update of fields and particles with charge-conserving and symplectic properties obtained from first principles. We study *multipactor* effects on different kinds of metal boundaries such as Cu and stainless steel and the saturation process due to a balanced competition between external RF potentials and space charges.

1 Introduction

Multipacting, which is a resonant electron discharge from conductor or dielectric surfaces, has been a troublesome factor in many high power RF devices [1, 2]. Once stray electrons traveling inside the device impact the device surface, the latter may re-emit single or multiple electrons, i.e. produce a secondary electron emission (SEE). If operating RF fields in the devices meet given resonant conditions the resulting electron population may grow exponentially inside the device, leading to potential damage. In the past, multipactor phenomena have been primarily studied via purely analytic or experimental approaches [2] since numerical solutions involving N-body Coulomb interactions are too burdensome. More recently, particle-in-cell (PIC) algorithms [3] have been increasingly used for a variety of space charge problems such as plasma physics or vacuum electronic devices. PIC algorithms lowers the $O(N^2)$ problem down to a $O(N)$ problem by considering forces acting on individual particles and the associated electromagnetic (EM) field in a collective way. In this summary paper, we conduct a numerical analysis of multipactor effects based on an irregular-grid-based particle-in-cell (PIC) algorithm [5, 6] We employ the probabilistic SEE model with a phenomenological approach [4] for a more realistic *multipactor* analysis rather than a conventional monoenergetic SEE model. Our PIC algorithm is exactly charge-conserving and symplectic and it yields a self-consistent time update of fields and particles [5, 6]. The use of irregular grids enables the accurate modeling of complex or locally-fine geometries found in modern high power devices, including geometrical surface treatments used to suppress multipactor effects [7]. To illustrate the capabilities of the algorithm, we provide numerical examples of multipactor effects on Cu and stainless steel plates and capture its saturation phenomenon.

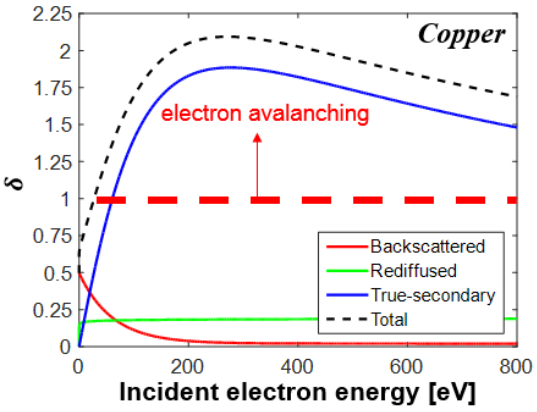

(a)

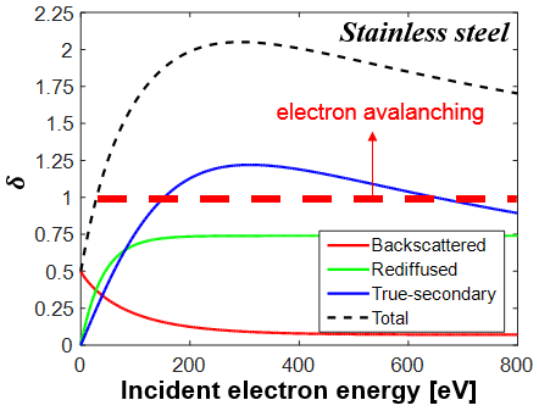

(b)

Figure 1. Secondary emission yield, δ versus incident electron energy for (a) copper and (b) stainless steel plates.

2 Irregular-Grid Charge-Conserving PIC Algorithm

PIC algorithms solve Vlasov equation describing the kinematics in collisionless plasma where the number density per Debye length is fairly dense. It tracks an evolution for

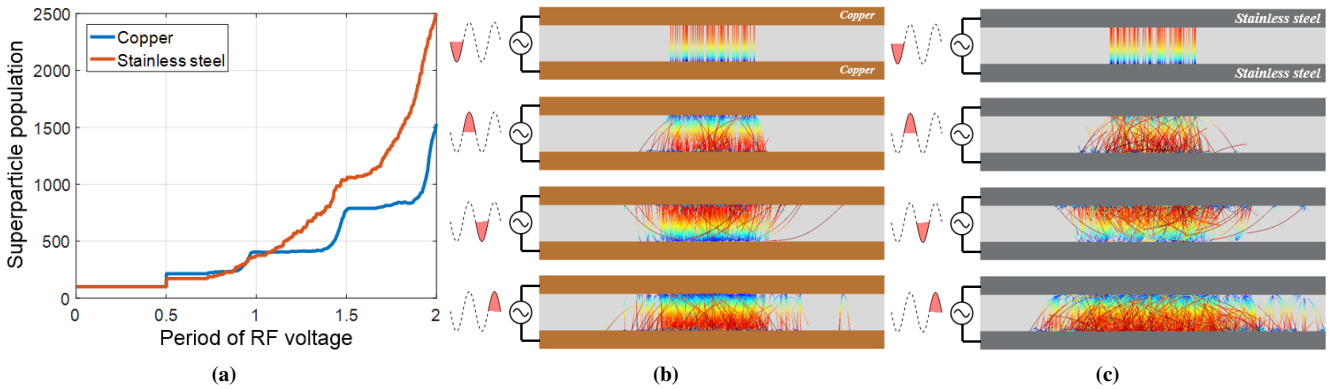

Figure 2. PIC results for probabilistic SEE model. (a) Superparticle population versus time (RF voltage periods). (b) and (c) Snapshots of particle's trajectories for Cu and stainless steel cases, respectively.

a finite-size ensemble of physical particles coarse-grained in phase space. Since moments of Vlasov equation become Newton-Lorentz equations of motion, resulting PIC algorithms can be constructed to solve time-dependent Maxwell's equation coupled to Newton-Lorentz equations of motion, while marching on time. There are four basic steps to be performed at each time-update on a PIC algorithm, viz. field-solver, gather, particle-push, and scatter. For the field solver, the present PIC algorithm adopts a finite-element method based on discrete exterior calculus [8, 9] whereby, starting from Maxwell's equations written in the language of *differential forms* [10, 11, 12], we expand field and source quantities by a weighted sum of Whitney forms [13, 14]. The gather step performs the field interpolation at each particle position again based on Whitney forms. Particles are accelerated by solving Newton-Lorentz equations of motion using Boris algorithm with correction [16, 17]. Present PIC algorithm achieves exact charge-conservation on irregular grids from first principle through a consistent use of Whitney forms again on the scatter step [5, 6].

3 Results and Discussion

We consider multipactor effects in a parallel plate system excited by an external RF voltage. The gap size between upper and lower plates, D equals to 0.002 m. We assume 100 seed superparticles, which are distributed as a tiny sheet near the lower plate, and launched with nonzero velocities. Each superparticle both as initial seeds and future secondaries represents about 2.5×10^8 electrons. The RF voltage applied to the plates has amplitude $V_0 = 300$ V and a frequency of $f = 1.044$ GHz. These parameters satisfy the resonant condition for multipacting in this device, which is given by $\omega D = (qV_0/m)^{1/2}$ where q and m are charge and mass of the superparticle, respectively, and ω is the angular frequency. According to the probabilistic SEE model [4], there are three types of SEE: backscattered (almost elastic), rediffused (partially elastic), and true-secondary (inelastic). One can refer to [4] for more details about each mechanism. Cu and stainless steel have different profiles of secondary emission yield (SEY), δ, which is the number of secondaries at given incident electron energy, as shown in Fig. 1. The parameter δ depends on the impact energy and electron avalanches occur if δ is larger than 1. Red, green, and blue solid lines denote δ by backscattered, rediffused, and true-secondary emissions, respectively, and the black dashed line is their aggregate. It can be seen that that true-secondary electrons dominate in Cu plates. As a result, most secondaries have low (kinetic) temperatures and are regularly accelerated to the retarding voltages. On the other hand, for the stainless steel plate, secondaries generated by rediffused emission process (partially elastic) increases about threefold compared to SEY of the Cu plate and true-secondary-based secondaries decreases as much. Results of PIC simulations with the probabilistic SEE model are shown in Fig. 2. Fig. 2a illustrates superparticle population versus RF voltage period for both Cu and stainless steel plates. In the Cu case, as expected, a nearly step-wise increase of the population can be observed whenever primary electrons hit the walls since the true-secondary emission process overwhelms the other processes. On the other hand, in the stainless steel case secondaries increase rather more gradually in population due to the balanced relationship between elastic and inelastic emissions. This is evidenced by the snapshots of particles' trajectory shown in Fig. 2b and Fig. 2c which plot particle's trajectories at each half period of the RF voltage for the two cases. The RGB color represents the kinetic energy of particles (red color represents more energetic particles). In order to capture the saturation phenomenon, we ran the simulation for 16 RF periods. Fig. 3 shows the number density against RF voltage cycle for the Cu case. The number density increases at an exponential rate up to an intermediate stage beyond which (about six RF cycles) a saturation state is reached. This saturation comes from the fact that secondary electrons are pulled back towards the surface by strong space-charge self-fields, as shown in an inset of Fig. 3. During the intermediate stage, the amplitude of RF fields prevail over the space-charge field, and most secondaries successfully escape from the emitted surface.

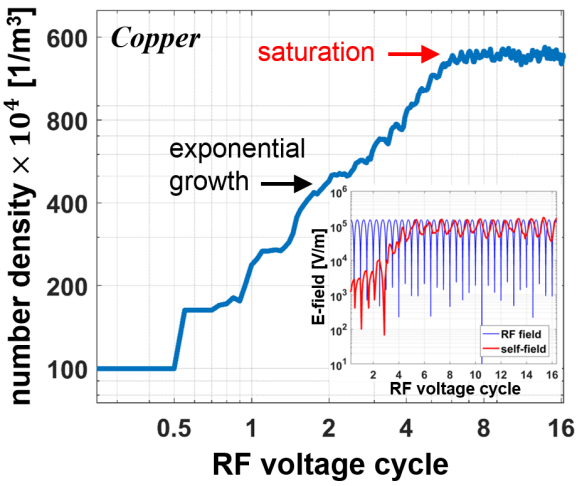

Figure 3. Number density of flight superparticles versus RF voltage cycle in Cu case.

4 Acknowledgements

This work was supported in part by U.S. NSF grant ECCS-1305838, OSC grants PAS-0061 and PAS-0110, and FAPESP-OSU grant 2015/50268-5. D.-Y. Na was also supported by the OSU Presidential Fellowship program.

References

[1] R. A. Kishek Y. Y. Lau, L. K. Ang, A. Valfells, and R. M. Gilgenbach, "Multipactor Discharge on Metals and Dielectric: Historical Review and Recent Theories," *Phys. Plasmas*, **5**, 5, April 1998, pp. 2120–2126, doi:10.1063/1.872883.

[2] J. R. M. Vaughan, "Multipactor," *IEEE Trans. Electron Devices*, **35**, 7, July 1988, pp. 1172–1180, doi:10.1109/16.3387.

[3] R. W. Hockney, J. W. Eastwood, Computer Simulation Using Particles, Institute of Physics Publishing, London, 1988.

[4] M. A. Furman and M. T. F. Pivi, "Probabilistic Model for the Simulation of Secondary Electron Emission," *Phys. Rev. ST Accel. Beams*, **5**, 12, December 2002, p. 124404, doi:10.1103/PhysRevSTAB.5.124404.

[5] H. Moon, F. L. Teixeira, Y. A. Omelchenko, "Exact Charge-Conserving Scatter-Gather Algorithm for Particle-in-Cell Simulations on Unstructured Grids: A Geometric Perspective," *Comput. Phys. Commun.*, **194**, September 2015, pp. 43–53, doi:10.1016/j.cpc.2015.04.014.

[6] D.-Y. Na, H. Moon, Y. A. Omelchenko, F. L. Teixeira, "Local, Explicit, and Charge-Conserving Electromagnetic Particle-in-Cell Algorithm on Unstructured Grids," *IEEE Trans. Plasma Sci.*, **44**, 8, August 2016, pp. 1353–1362, doi:10.1109/TPS.2016.2582143.

[7] M. T. F. Pivi, F. K. Kind, R. E. Kirby, T. O. Raubenheimer, G. Stupakov, and F. Le Pimpec, "Sharp Reduction of the Secondary Electron Emission Yield from Grooved Surfaces," *J. Appl. Phys.*, **104**, November 2008, p. 104904, doi:10.1063/1.3021149.

[8] F. L. Teixeira and W. C. Chew, "Lattice Electromagnetic Theory from a Topological Viewpoint," *J. Math. Phys.*, **40**, 1, January 1999, pp. 169–187, doi:http://dx.doi.org/10.1063/1.532767.

[9] B. He and F. L. Teixeira, "On the Degrees of Freedom of Lattice Electrodynamics," *Phys. Lett. A*, **336**, 1, January 2005, pp. 1–7, doi:10.1016/j.physleta.2005.01.001.

[10] B. He and F. L. Teixeira, "Differential Forms, Galerkin Duality, and Inverse Sparse Approximations in Finite Element Solutions of Maxwell Equations," *IEEE Trans. Antennas Propagat.*, **55**, 5, May 2007, pp. 1359–1368, doi:10.1109/TAP.2007.895619.

[11] R. Rieben, G. Rodrigue, and D. White, "A High Order Mixed Vector Finite Element Method for Solving the Time Dependent Maxwell Equations on Unstructured Grids," *J. Comp. Phys.*, **204**, 2, March 2004, pp. 490–519, doi:705 10.1016/j.jcp.2004.10.030.

[12] F. L. Teixeira, "Lattice Maxwell's Equations," *Prog. Electromagn. Research*, **148**, July 2014, pp. 113–128, doi:10.2528/PIER14062904.

[13] B. He, F. L. Teixeira, "Geometric Finite Element Discretization of Maxwell Equations in Primal and Dual Spaces," *Phys. Lett. A* **349**, 1-4, January 2006, pp. 1-14, doi:10.1016/j.physleta.2005.09.002.

[14] B. Donderici and F. L. Teixeira, "Mixed Finite-Element Time-Domain Method for Transient Maxwell Equations in Doubly Dispersive Media," *IEEE Trans. Microw. Theory Tech.*, **56**, 1, January 2008, pp.113–120, doi:10.1109/TMTT.2007.912217.

[15] J. Kim and F. L. Teixeira, "Parallel and Explicit Finite-Element Time-Domain Method for Maxwell's Equations," *IEEE Trans. Antennas Propag.*, **59**, 6, June 2011, pp. 2350–2356, doi:10.1109/TAP.2011.2143682.

[16] J. P. Verboncoeur, "Particle Simulation of Plasmas: Review and Advances," *Plasma Phys. Control. Fusion*, **47**, April 2005, pp. A231–A260, doi:10.1088/0741-3335/47/5A/017.

[17] J.-L. Vay, "Simulation of Beams or Plasmas Crossing at Relativistic Velocity," *Phys. Plasmas*, **15**, February 2008, p. 056701, doi:10.1063/1.2837054.